The Kombucha Biofilm: a Model System for Microbial Ecology

Ashley Shade
Gordon and Betty Moore Foundation Fellow of the Life Sciences Research Foundation
Yale University

27 July 2011
Final report on research conducted during the Microbial Diversity course, Marine Biological Laboratories, Woods Hole, MA

Abstract

Microbial systems are inherently complex and difficult to predict. A strong model system of naturally-occurring microbial consortia would provide opportunity to address key questions in microbial ecology. Kombucha is a traditional, fermented tea produced by a biofilm of yeast and acetic acid producing bacteria. Because it has well-defined functional products and is maintained easily at the laboratory-scale, kombucha has potential as a mixed-microbial model system. I provide a first exploration of the kombucha system for microbial ecology. I first describe the kombucha microbial consortia using isolation and 16S 454 tag-pyrosequencing. I assessed the temporal dynamics of kombucha by tracking microbial abundance and key products from inoculation to culture maturation. Then, I observed the spatial structure and association of abundant organisms with each other in the cellulose matrix of the biofilm using confocal microscopy. Finally, I designed an experiment to assess the influence of pH and tea origin on the consortia and their products. I found that kombucha habours a dominant *Glucoacetobacter* population, and uncovered evidence for more resolved population-level diversity within the biofilm. Cell counts of the kombucha broth peaked at pH 3 on day 3 after innoculation, indicating that the acid concentration of the peak may provide a strong environmental filter for the microbes. The biofilm was heterogeneous in space, containing patches of yeast within a matrix of cellulose and segregated bacterial cells. Finally, tea origin and pH partially determine the rate of product evolution in kombucha broth, and tea may inhibit the growth of the consortia. This work lays a foundation for using kombucha as a model system for microbial ecology.

Introduction

Microbial systems are inherently complex. A key challenge is to understand the biotic and abiotic interactions of microbial systems to the endpoint of prediction (Prosser et al., 2007). However, many microbial systems found in nature are difficult to manipulate experimentally and have under-described diversity as well as many unknown or intractable functions (Jessup et al., 2004). On the other hand, many model laboratory systems, in microbiology and other fields, are arguably over-simplified, maintained in controlled conditions generally unrealistic to naturally occurring systems (e.g. (Carpenter and Url, 2011)). Though both environmental and lab-scale systems are important for understanding different aspects of microbial complexity, a relatively simple, authentic model microbial system is desirable for lab scale manipulations. Such a tractable model would advance theory and achieve progress towards prediction in microbial ecology.

Kombucha is a beverage of fermented tea consumed traditionally in eastern Europe and Asia. To prepare kombucha, black tea leaves are seeped in boiling water, copious amounts of sugar (sucrose) is added, and the mixture is cooled to room temperature. Then a "mother" biofilm is placed into the tea; this biofilm is sometimes called a symbiotic culture of bacteria and yeasts (SCOBY), and is comprised of acetic acid producing bacteria, ethanol fermenting yeasts, and a thick cellulose pellicle. This starter biofilm, or unpasteurized liquid from an active kombucha culture, is necessary to begin kombucha production. The biofilm floats at the liquid-air interface and grows vertically, increasing biomass with cellulose striations as the fermentation matures. After several days incubation at room temperature, the tea becomes a sweet and sour, naturally carbonated beverage because of microbial activities. Kombucha has been both sanctioned and advocated as a health beverage, with no consensus (Dufresne, 2000). However, kombucha consumption is gaining popularity worldwide, and there is much interest in scaling up the fermentation process to meet food industry demands (e.g. (Chen and Liu, 2000; Malbasa et al., 2006; Cvetkovic et al., 2008; Jayabalan et al., 2008)).

The general products of kombucha fermentation are sugars and organic acids. The yeasts convert sucrose to glucose and fructose during fermentation, as a byproduct of ethanol fermentation(Blanc, 1996). The acetic acid producing bacteria then convert fructose into acetic acid (which provides kombucha with its sour flavor) and glucose to gluconic acid. Accordingly, the pH of the enrichment drops to approximately 2.6 after, signifying the maturation of the beverage for consumption. If the fermentation is not stopped or slowed, the gluconic and acetic acid concentrations will continue to increase to levels of (4 g/100 mL, (Chen and Liu, 2000)), but the beverage will be intolerable for consumption because of a strong vinegar flavor. An additional byproduct of acetic acid production by bacteria is cellulose (Iguchi et al., 2000), which provides scaffold to the biofilm-associated microbes.

Because the kombucha biofilm is a mixed eukaryotic-bacterial microbial community and has clear functions and products, it may serve as an excellent study system for microbial ecology. There has been identification of some of the yeast and bacterial species found in various SCOBYs. It was found that the species composition of kombuchas vary by biofilm origin, especially with respect to the associated yeast

species (Teoh et al., 2004). However, the “vertically” transferred nature of biolfilms among kombucha producers raises interesting questions about biogeography, selection and evolution. Additionally, many specific interactions between the yeast and bacteria are unknown, including the mechanisms of biofilm formation from pelagic cells, the nature of the symbiosis between the eukaryotic and prokaryotic components (e.g. do the acetic acid bacteria have an obligate relationship the yeast?), or the cellular and cellulosic architecture of the biofilm. Genetics of the system (with the exception of species identifications using common molecular markers, e.g. (Kurtzman et al., 2001; Dutta and Gachhui, 2007)) is also a dearth. Indeed, much of the basic microbial ecology of the kombucha system is undocumented. Yet ease of lab-scale culturing and manipulation (the biofilm grows well and quickly at room temperature with minimal specialized equipment), kombucha has potential as a naturally occurring, simple, and authentic model for microbial communities and their interactions.

Here, I provide a first exploration of the utility of kombucha microbial community as a model system. Using a combination of classical microbiology with molecular tools, I describe temporal and spatial dynamics of kombucha, from inoculation to culture maturation. I also conducted an experiment to understand the influence of tea origin and pH on the microbial products of kombucha.

Materials and Methods

i. Enrichment and isolation conditions

The starter culture of kombucha had been maintained for approximately one year at home. Teas were from Upton Tea Imports (http://www.uptontea.com). To prepare tea media, milliQ water was boiled, and 5 g tea per liter was seeped for 10-15 minutes. Tea leaves were removed from liquid before autoclaving. Afterwards, sucrose was added to a final w/v concentration of 15%. Oolong (brown) tea (10 mL final volume in capped culture tubes) was used for the time series observations. Oolong, Ceylon black tea, and green tea were used for the tea comparison experiment (90 mL final volume in sample jars covered but not sealed with caps), as well as freshwater minimal medium and oolong tea amended with MOPS pH 6.2-7 buffer. The freshwater medium broth contained vitamins while the plates did not. Calcium carbonate plates to identify acid producers by halo formation was prepared according to (Chen and Liu, 2000): 30 g glucose, 5 g yeast extract, 3 g peptone, 10 g calcium carbonate, and 30 mL of 95% ethanol, added after autoclaving, 20 g agar, and sterile milliQ water to 1 L. Tea agar plates were prepared as above, but 15 g of agar was added prior to autoclaving. Media was inoculated with 10% v/v of kombucha broth from a previous culture. Liquid cultures were incubated at room temperature; plates were incubated at 30 C.

ii. pH and organic acids measurements

Acid (pH) was measured daily and the probe was calibrated at each use.

Samples for organic acid analysis on HPLC were prepared from 1 mL of broth. Cells were pelleted and supernatant filtered through a 0.2 micron Acrodisc syringe filter (Pall), and then acidified with 100 uL 5 M sulfuric acid. Organic acids analysis was performed on a Shimadzu LC-2010C System with an RID detector and an Aminex HPX-

87H column (BioRad). Pump flow was 0.6 mL/min at minimum pressure 0 psi and maximum 1422 psi, autosampling 20 uL, oven temperature at 60 C, and a 30 minute program duration. Calibrations for ethanol ranged from 1.0 to 50 mM, acetic acid ranged from 1.0 to 100 mM, glucose from 1.0 to 500 mM, fructose from 1.0 to 300 mM, and lactose from to 30 mM. The method was called “Alexa Organic acids- Ashley modified.”

iii. Molecular tools

DNA was isolated from two independent kombucha biofilms using the UltraClean Soil DNA Isolation kit (MoBio), as per manufacturer’s instructions with minor modifications. The biofilms were from 10 mL 20 day Irish Breakfast and a 13 day Oolong cultures. Biofilms were cut with a sterile razor blade into small pieces and bead beat for 1 minute. The optional 65 C incubation was performed to increase yield.

16S sequencing of isolates was performed using bacterial primer set 8F and 1492R with Promega Master Mix as per manufacturer’s instructures. Thermocycler conditions were: 5 min boil (95 °C), 5 min denaturation 95 °C, 30 cycles of 95 °C 30 s denaturation, 46 °C 30 s annealing, 72 °C 1.5 m extension, followed by a final extension for 5 m at 72 °C and a hold at 4 °C. PCR clean-up was performed using MinElute columns as per manufacturer’s instructions (Qiagen). Twenty ng/uL were submitted for sequencing

Tag-pyrosequencing was performed on two independent biofilms. The first biofilm was 20 days old and grown in Irish Breakfast tea, the second was 13 days old and grown in oolong tea. Both cultures were 10 mL and ~15% sucrose.

SU rRNA genes were amplified with barcoded primers that also incorporated the roche 454 Ti adapter sequences, with the barcode on the forward primer. Each barcode was 9 nt long and all the barcodes we used are in the mapping file for the 454 data on dropbox. The primer targets 515F and 907R on the *E. Coli* 16S gene. The forward primer was (X denotes barcode, lowercase is the linker between barcode and 16S primer):

5'-
CGTATCGCCTCCCTCGCGCCATCAGXXXXXXXXgaGTGYCAGCMGCCGCGGTAA-3'

The reverse primer was (lowercase denotes linker between adapter and 16S primer):
5'-CTATGCGCCTTGCCAGCCCGCTCAGggCCGYCAATTCMTTTRAGTTT-3'

Phusion HF polymerase (2X MasterMix) was used to amplify the gene with 8% DMSO and 0.5 uM primers in the final reaction volume. Template was normalized to 15 ng/uL. Touchdown PCR program annealing temperature was from 58-58 C for the first 10 cycles, followed by 12 cycles of three-step PCR (denaturation, annealing, elongation) and 10 cycles of two-step PCR. DNA was quantified using the PicoGreen and pooled ~125 ng each PCR product. That pool was concentrated down 100 uL and gel purifed using the Montage Kit (Millipore). The gel-purified pool was sequenced by the Penn State sequencing facility.

Analyses of the 454 data were performed using the QIIME workflow (Caporaso et al., 2010), with quality control for minimum length 400 bp, maximum length 600 mp, no primer mismatches, and a minimum quality score of 25. Clusters were defined at 97 and

100% sequence identity using CD-HIT (Li and Godzik, 2006). Taxonomic assignments were made with RDP. Species abudnace distribution models were fit using the vegan package in the R environment for statistical computing (R Development Core Team, 2010)(Team", 2010).

iii. Microscopy

Dead cell staining was performed on live biofilm cross sections (manually prepared with a sterile razor blade) using propidium iodide (Invitrogen) as per manufacturer's instructions.

Broth from kombucha cultures were fixed overnight in 1% final concentration of paraformaldehyde at 4 °C or 1-4 hours at room temperature. 150 uL of the broth was filtered through 0.22 polycarbonate filters (Nucleopore, Pall). Filters were store at -20 until further processing. Visualization of cells by DAPI staining were performed on slices of filters by washing in 1 ug/mL of DAPI solution for 5-15 minutes, washing in sterile milliq water for 10 minutes, washing in ethanol for 5 minutes, and then air drying in the dark. Filters were mounted in a 75:25 Citifluor: VectraShield solution and visualized with epifluorescence microscopy. CARD-FISH was performed according to (Pernthaler et al., 2004) using the Alf968 probe for Alpha-Proteobacteria and Alexa 488 tyramide.

Confocal images were from a Zeiss LSM-700 microscope.

iv. Experimental design

The tea and pH experiment included five treatments with three replicates each, followed for eleven days. The treatments were different media, including oolong, Ceylon, and green teas, oolong tea buffered with MOPs, and FWC liquid media. Acid was measured daily and 1 mL of broth collected for HPLC analysis and stored at -20 until further processing. On the final day, depth of the biofilm at the thickest point was measured, and samples were preserved for future molecular analysis of community composition.

Results and Discussion

i. Composition

Isolation uncovered four different colony morphologies from the kombucha, including yeast and bacteria (**Figure 1**). All isolates were submitted for 16S sequencing, but only isolate Kmbch_06 had a quality sequence and was preliminarily identified as a *Gluconacetobacter* species. Notably, not all bacterial isolates produced acid, as assayed by halo formation on the calcium carbonate plates.

Tag pyrosequencing resulted in 36,414 quality sequences (SCOBY 1 = 18,699 tags, SCOBY 2 = 17,715 tags), and 131 OTUs at the 97% sequence identity clusters using CD-HIT. Of these OTUs, 26 were non-singleton OTUs and 8 of these were assigned to the *Gluconacetobacter* genus. Species abundance distributions revealed a few dominant OTUs (all *Gluconacetobacter)* with many singletons in both SCOBYs (**Figure 2**). Few OTUs were identified that were not either *Gluconacetobacter* or belonging to the Acetobacteraceae family. These included a few chloroplast (likely form the tea), and also OTUs identified with Alteromonadaceae, Halomonadacae *Halomonas*, Spirochaetacea *Spirochaeta*, Staphylococcaceae *Staphylococcus*,

Streptococcaceae *Streptococcus*, Bacillariophyta, and Desulfobacteraceae. These OTUs may represent flanking rare members of the kombucha community.

To further probe population-level diversity within the *Gluconacetobacter*, OTUs were clustered at 100% sequence similarity, resulting in 2854 OTUs and 2697 of these were identified as *Gluconacetobacter.* Alignments of the tag-sequences revealed that many of these OTUs were different in a single base pair within the tag-sequences (which were 414 bp in length). A one to one plot of the independent SCOBY samples revealed that the abundances of *Gluconacetobacter* OTUs were very consistent across samples, suggesting that the patterns in population-level diversity are not due to random sequencing error (**Figure 3**). This also suggests that there is low compositional variability between mature SCOBY communities. Consideration of the ten most abundant *Gluconacetobacter* OTUs supported this consistency across samples (**Table 1**).

A local database of the 100% identity OTUs was created, and isolate 16S sequences of was BLASTed against this to determine if one of the abundance OTUs had been isolated. Surprisingly, Kmbch_06 isolate, the acid producer with small colonies in **Figure 1c and 1g** had 100% identity in the overlapping region to OUT 1973, which was a singleton sequence in the dataset.

These results show that while there is low bacterial community diversity in kombucha, there is strong evidence for high population-level diversity. The differences in phenotypes, especially isolating bacteria that produces cellulose and another that produces acid, suggests some complementation of roles of *Gluconacetobacter* in the biofilm.

ii. Temporal and spatial dynamics of kombucha

CARD-FISH with Alf968 probe was used to determine the proportion of Alpha-Proteobacteria in the kombucha broth. Samples used for this analysis were replicate 10 mL cultures of 15% Oolong, sacrificed daily. No unlabeled cells were detected, suggesting that the majority of cells were alphas. Therefore, DAPI staining was used to count cells from the time series and identify Eukaryotes by nuclear staining (**Figure 4**). Total cells in the broth peaked on day 3 after inoculation, suggesting some inhibition of growth of planktonic populations, possibly because of increased acid or other antimicrobial products.

A series of confocal images through the horizontal axis of the biofilm was observed using DIC imaging with propidium iodide dead cell staining (**Supplemental Material: Confocal Z stacks movie**). This revealed high spatial heterogeneity within the biofilm, as there were patches of dead *Acetobacter*-like cells, unstained *Acetobacter*-like cells throughout the cellulose matrix, and patches of unstained yeast cells on a different plane. These results suggest that the yeast and *Gluconacetobacter* are not physically associated with each other within the biofilm, but that the biofilm may have specific compartments for functions (e.g. ethanol fermentation by yeast).

iii. The influence of pH and tea type on kombucha function

I designed an experiment to better understand the temporal dynamics of the microbial products in kombucha given different tea origins and acidities. Also I asked whether enrichment on tea was essential for kombucha microbes by inoculating

freshwater minimal media (FW) with kombucha broth. There were five treatments with three replicates each: Ceylon black tea, green tea, oolong tea, oolong tea buffered with MOPS (range 6.5-7.9), and freshwater minimal media. Ninety milliliter enrichments were used, and broth was removed each day for eleven days to measure pH and organic acids. On the final day, biofilm thickness was measured as a proxy for cellulose production.

pH steadily decreased in all of the treatments, but the oolong buffered mops maintained higher pH than the others (**Figure 5**). The pH remained lowest in the FW treatment, I observed that the biofilm formed most rapidly. The different tea types were similar in their pH dynamics.

Organic acids analysis of non-inoculated control media showed that all of the media were very similar in initial lactose and fructose concentrations, but that the FW media had higher initial glucose than the others (**Figure 6a**). Because all media were prepared with 15% sucrose, these concentrations of simpler sugars are likely due to natural breakdown from specific media conditions. Ethanol was produced immediately and gradually in all of the treatments (**Figure 6b**). Ceylon tea had the most ethanol production by the end of the time series, twice as concentrated as the other treatments. FW ethanol increased most slowly, but by day 10 matched the concentrations of the other treatments (except for Ceylon). Acetic acid was not produced in significant quantities until day 5 (**Figure 6c**), suggesting that a minimum threshold of ethanol (resulting in sucrose degradation to fructose and glucose) may be required before *Gluconacetobacter* could begin acetic acid production. Further, it makes sense that the *Gluconacetobacter* would grow more quickly given simpler carbon sources. The most acetic acid was produced in the FW treatment, and the least in the oolong MOPS-buffered tea. The former suggests the hypothesis that tea may inhibit growth of *Gluconacetobacter*, leading to a decrease in acid production. Lactose concentrations were most dynamic in time, with a gradual drop until day 3 and then a sharp increase by day 5, followed by another drop to day 10 (**Figure 6d**). However, these dynamics were consistent across all treatments. These data suggests a hypothesis that there may have been an increase in flanking lactic acid producing bacteria that were later outcompeted by *Gluconacetobacter*. Note, however, the generally low concentrations (y axis) in lactic acid throughout. Analysis of the community composition through the time series would be necessary to test this hypothesis. Glucose dynamics, however were not consistent across treatments (**Figure 6e**). Oolong buffered with MOPs had twice as much glucose than the other treatments throughout the experiment. Fructose gradually decreased in all treatments (**Figure 6f**), though the magnitude was much less in the MOPS buffered oolong.

Biofilm thickness was consistent across treatments, however the oolong treatment was much more variable than the others and the FW treatment had a greater thickness (**Figure 7**). Future work should measure dry biomass as a better proxy for cellulose production in the biofilm.

Conclusions

My preliminary explorations of the microbial ecology of the kombucha biofilm have only created more questions. I have shown that kombucha is dominated by *Gluconacetobacter*, and that there is phenotypic and functional diversity in isolate (some

produce more acid, some produce more cellulose). I have demonstrated by DAPI counts that the abundance of pelagic community changes in time, and by confocal microscopy with propidium iodide staining that there is high spatial heterogeneity in the biofilm. In my “tea experiment”, I showed that pH and tea origin separately play a role in the dynamics of known products of the kombucha consortia, and also that the tea is not required for kombucha biofilm formation, as the biofilm in the FW treatment grew even thicker (more cellulose production) than the other treatments, despite that the acetic acid production remained low and glucose remained high. An interesting finding was in the population-level diversity within the Gluconacetobacter OTUs observed with deep 454-sequencing (arguably exhaustive for this simple bacterial consortia). Full 16S and/or rpoB sequencing of isolates from the kombucha would help to address the question of how much diversity exists within *Gluconacetobacter*, and what environmental or biological factors may drive this diversity. Another interesting unknown is the identity of yeast species in kombucha; isolation and sequencing of the yeast will provide a foundation for understanding Eukaryotic- bacterial interactions in the kombucha consortia.

Acknowledgements
A.S. is a Gordon and Betty Moore Foundation Fellow of the Life Sciences Research Foundation. Funds for participation in Microbial Diversity were provided by the Life Sciences Research Foundation fellowship to AS, the American Society for Microbiology Early Career Development Grant for Postdoctoral Women to AS, and National Science Foundation grant to the Microbial Diversity course (Buckley and Zinder).

References

Blanc, P.J. (1996) Characterization of the tea fungus metabolites. *Biotechnology Letters.***18**: 139-142.

Caporaso, J.G., Kuczynski, J., Stombaugh, J., Bittinger, K., Bushman, F.D., Costello, E.K. et al. (2010) QIIME allows analysis of high- throughput community sequencing data. *Nature.* **7**: 335-336.

Carpenter, S.R., and Url, S. (2011) Microcosm Experiments have Limited Relevance for Community and Ecosystem Ecology. *Ecology.* **77**: 677-680.

Chen, C., and Liu, B.Y. (2000) Changes in major components of tea fungus metabolites during prolonged fermentation. *Journal of Applied Microbiology.* **89**: 834-839.

Cvetkovic, D., Markov, S., Djuric, M., Savic, D., and Velicanski, a. (2008) Specific interfacial area as a key variable in scaling-up Kombucha fermentation. *Journal of Food Engineering* **85**: 387-392.

Dufresne, C. (2000) Tea, Kombucha, and health: a review. *Food Research International* **33**: 409-421.

Dutta, D., and Gachhui, R. (2007) Nitrogen-fixing and cellulose-producing Gluconacetobacter kombuchae sp. nov., isolated from Kombucha tea. *International journal of systematic and evolutionary microbiology* **57**: 353-357.

Iguchi, M., Yamanaka, S., and Budhiono, A. (2000) Bacterial cellulose—a masterpiece of nature's arts. *Journal of Materials Science* **35**: 261-270.

Jayabalan, R., Marimuthu, S., Thangaraj, P., Sathishkumar, M., Binupriya, A.R., Swaminathan, K., and Yun, S.E. (2008) Preservation of kombucha tea-effect of temperature on tea components and free radical scavenging properties. *Journal of agricultural and food chemistry* **56**: 9064-9071.

Jessup, C.M., Kassen, R., Forde, S.E., Kerr, B., Buckling, A., Rainey, P.B., and Bohannan, B.J.M. (2004) Big questions, small worlds: microbial model systems in ecology. *Trends in Ecology & Evolution* **19**: 189-197.

Kurtzman, C.P., Robnett, C.J., and Basehoar-Powers, E. (2001) Zygosaccharomyces kombuchaensis, a new ascosporogenous yeast from 'Kombucha tea'. *FEMS yeast research* **1**: 133-138.

Li, W., and Godzik, A. (2006) Cd-hit: a fast program for clustering and comparing large sets of protein or nucleotide sequences. *Bioinformatics* **22**: 1658.

Malbasa, R., Loncar, E., Djuric, M., Klasnja, M., Kolarov, L., and Markov, S. (2006) Scale-Up of Black Tea Batch Fermentation by Kombucha. *Food and Bioproducts Processing* **84**: 193-199.

Pernthaler, A., Pernthaler, J., and Amann, R. (2004) Sensitive multi-color fluorescence in situ hybridization for the identification of environmental microorganisms. *Molecular microbial ecology manual, 2nd ed Kluwer Academic Publishers, Dordrecht, The Netherlands*: 711-726.

Prosser, J.I., Bohannan, B.J.M., Curtis, T.P., Ellis, R.J., Firestone, M.K., Freckleton, R.P. et al. (2007) The role of ecological theory in microbial ecology. *Nature Reviews Microbiology* **5**: 384-392.

R Development Core Team (2010) R: A language and environment for statistical computing. In. Vienna, Austria: R Foundtation for Statistical Computing.

Teoh, A.L., Heard, G., and Cox, J. (2004) Yeast ecology of Kombucha fermentation. *International Journal of Food Microbiology* **95**: 119-126.

Figure Legends

Figure 1. Colony and cell morphologies of representative isolates from kombucha. **a)** Yeast isolate on calcium carbonate plate with glucose and ethanol; **b)** Acetobacter-like isolate on calcium carbonate plate, globs are likely cellulose; **c)** Acid-producing isolate on calcium carbonate plate; **d)** Acetobacter-like isolate on FWC plate without vitamins, globs are almost 1 mm high and are likely cellulose; **e)** DIC image reveals cell morphology of yeast isolate in (a); f) Phase contrast reveals of cell morphology of bacterial isolate in (b), long rods occurring in pairs; **g)** Phase contrast image cell morphology of bacterial isolate from (c), squat rods occurring in pairs; **h)** Phase contrast image of cell morphology of bacterial isolate from (d), long rods in pairs or chains with bulbs, arrow shows likely cellulose fibers. White bars are 10 microns, e-h are 100x.

Figure 2: Species abundance distributions of SCOBY 1 and SCOBY 2. No model tested (lognormal, preemptive, Zipft, Zipft-Mandelbrodt, Null) fit well to the distribution.

Figure 3. SCOBY 1 and SCOBY 2 comparison of abundances of tag-pyrosequences from OTUs identified most closely as *Gluconacetobacter* using 100% clustering of tag-pyrosequences with CD-HIT in the QIIME workflow. A linear model revealed a significant 1:1 relationship, indicating that most OTUs were equally represented in both biofilms.

Figure 4. Cell counts by DAPI staining through time. **a)** DAPI and **b)** CARD-FISH with alpha-Proteobacteria probe Alf968 and Alexa 488 was used to confirm that all observed bacterial cells observed belong to alpha-Proteobacteria. Therefore, DAPI was used for total cell counting and identification of Eukaryotes by nuclear staining. **c)** Blue bars are total cell counts (bacteria and Eukaryotes), and red bars are total Eukaryotic cells.

Figure 5. pH dynamics of different treatments to understand the influence of tea origin and pH on the kombucha microbial consortia. Error bars are standard deviations around the mean of three replicates per time point per treatment.

Figure 6. Organic acids analysis by HPLC to understand the influence of tea origin and pH on the kombucha microbial products. **a)** Initial control concentrations of sugars. No acetic acid or ethanol was detected in the controls. **b)** Ethanol; **c)** acetic acid; **d)** lactose; **e)** glucose; **f)** fructose concentrations through time. Error bars are standard deviations around the mean of three replicates per time point per treatment.

Figure 7. Thickness of biofilms formed by the end of eleven days, as a proxy for cellulose production and biofilm growth. Measurements were at the thickest point in the biofilm.

Table 1. Ten most abundant OTUs identified as *Gluconacetobacter*, clustered at 100% tag-pyrosequence identity using CD-HIT. Sequences are available in supplemental information.

OTU ID	No. sequences SCOBY 1	No. sequences SCOBY 2	Representative sequence ID
1095	1011	1037	ASB1_27557
627	860	858	ASB1_27505
1089	690	733	ASB1_27517
1088	696	670	ASB1_27509
517	634	685	ASB1_27522
1101	684	607	ASB1_27641
39	565	635	ASB1_27533
1092	536	483	ASB1_27534
1087	499	503	ASB1_27507
1020	537	434	ASB1_27540

Supplemental material: movie of series of biofilm DIC propidium iodide stain, along the horizontal axis of the biofilm. Propidium idodide stains dead cells. The movie shows patches of dead *Acetobacter*-like cells, unstained *Acetobacter*-like cells throughout the cellulose matrix, and unstained yeast patches on a separate plane.

Figure 1

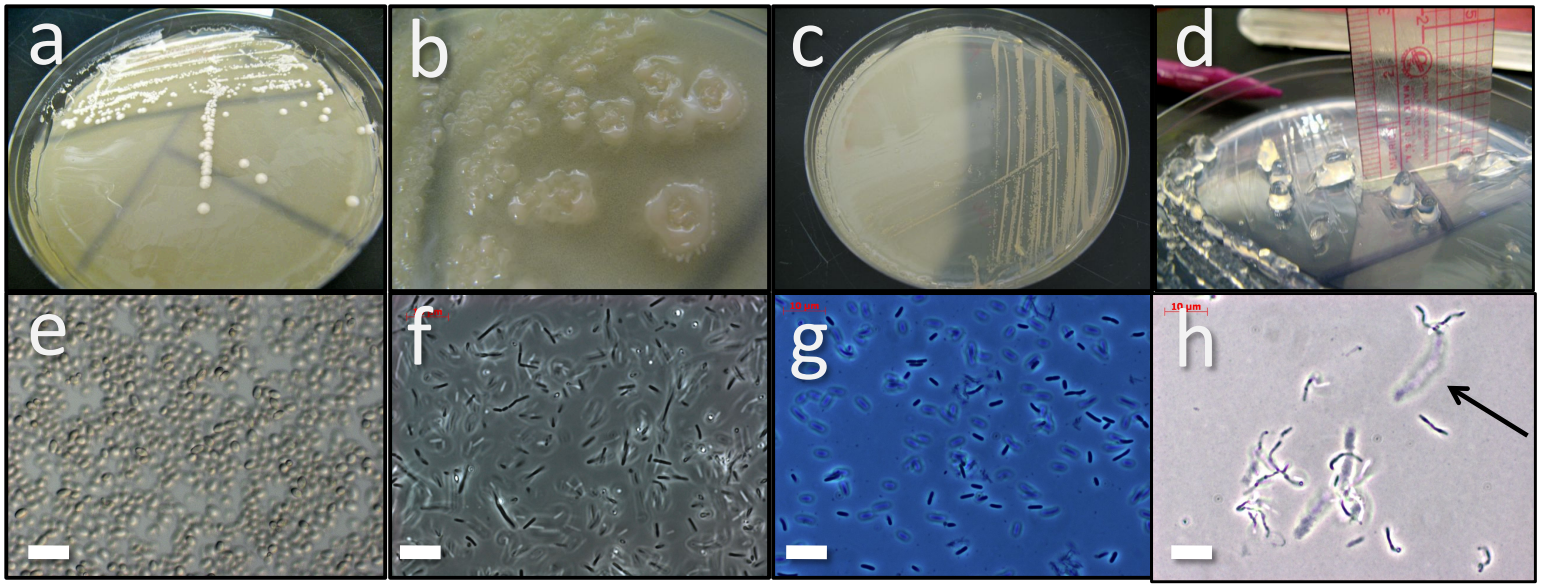

Figure 1. Colony and cell morphologies of representative isolates from kombucha. **a)** Yeast isolate on calcium carbonate plate with glucose and ethanol; **b)** Acetobacter-like isolate on calcium carbonate plate, globs are likely cellulose; **c)** Acid-producing isolate on calcium carbonate plate; **d)** Acetobacter-like isolate on FWC plate without vitamins, globs are almost 1 mm high and are likely cellulose; **e)** DIC image reveals cell morphology of yeast isolate in (a); f) Phase contrast reveals of cell morphology of bacterial isolate in (b), long rods occurring in pairs; **g)** Phase contrast image cell morphology of bacterial isolate from (c), squat rods occurring in pairs; **h)** Phase contrast image of cell morphology of bacterial isolate from (d), long rods in pairs or chains with bulbs, arrow shows likely cellulose fibers. White bars are 10 microns, e-h are 100x.

Figure 2

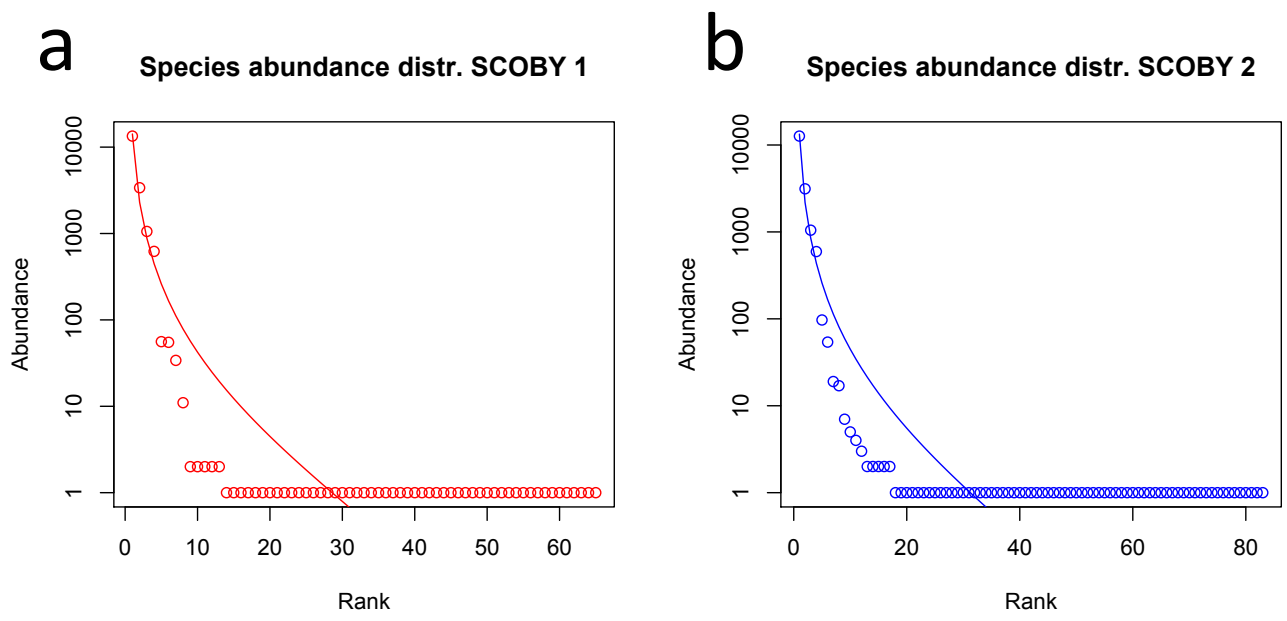

Figure 2: Species abundance distributions of SCOBY 1 and SCOBY 2. No model tested (lognormal, preemptive, Zipft, Zipft-Mandelbrodt, Null) fit well to the distribution.

Figure 3

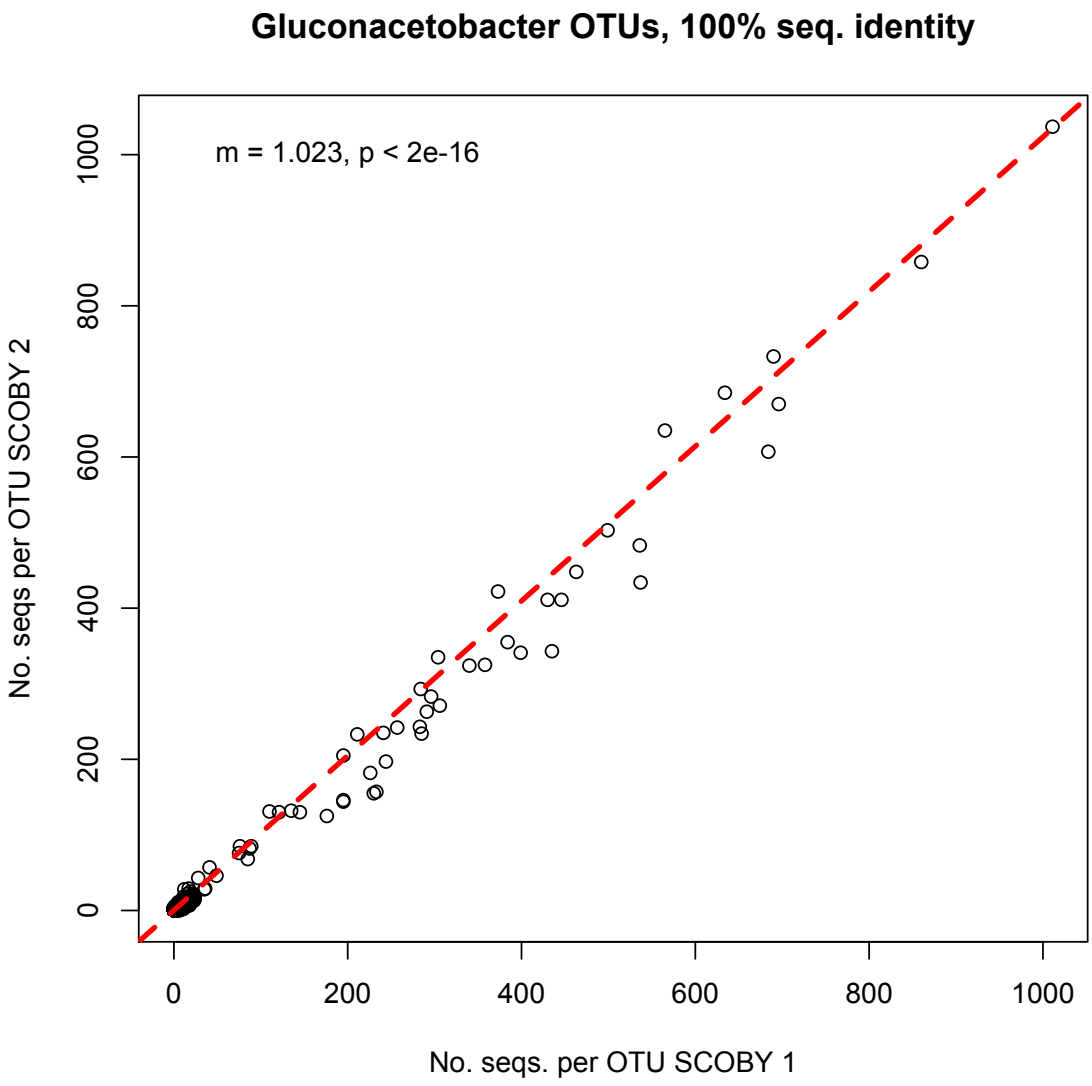

Figure 3. SCOBY 1 and SCOBY 2 comparison of abundances of tag-pyrosequences from OTUs identified most closely as *Gluconacetobacter* using 100% clustering of tag-pyrosequences with CD-HIT in the QIIME workflow. A linear model revealed a significant 1:1 relationship, indicating that most OTUs were equally represented in both biofilms.

Figure 4

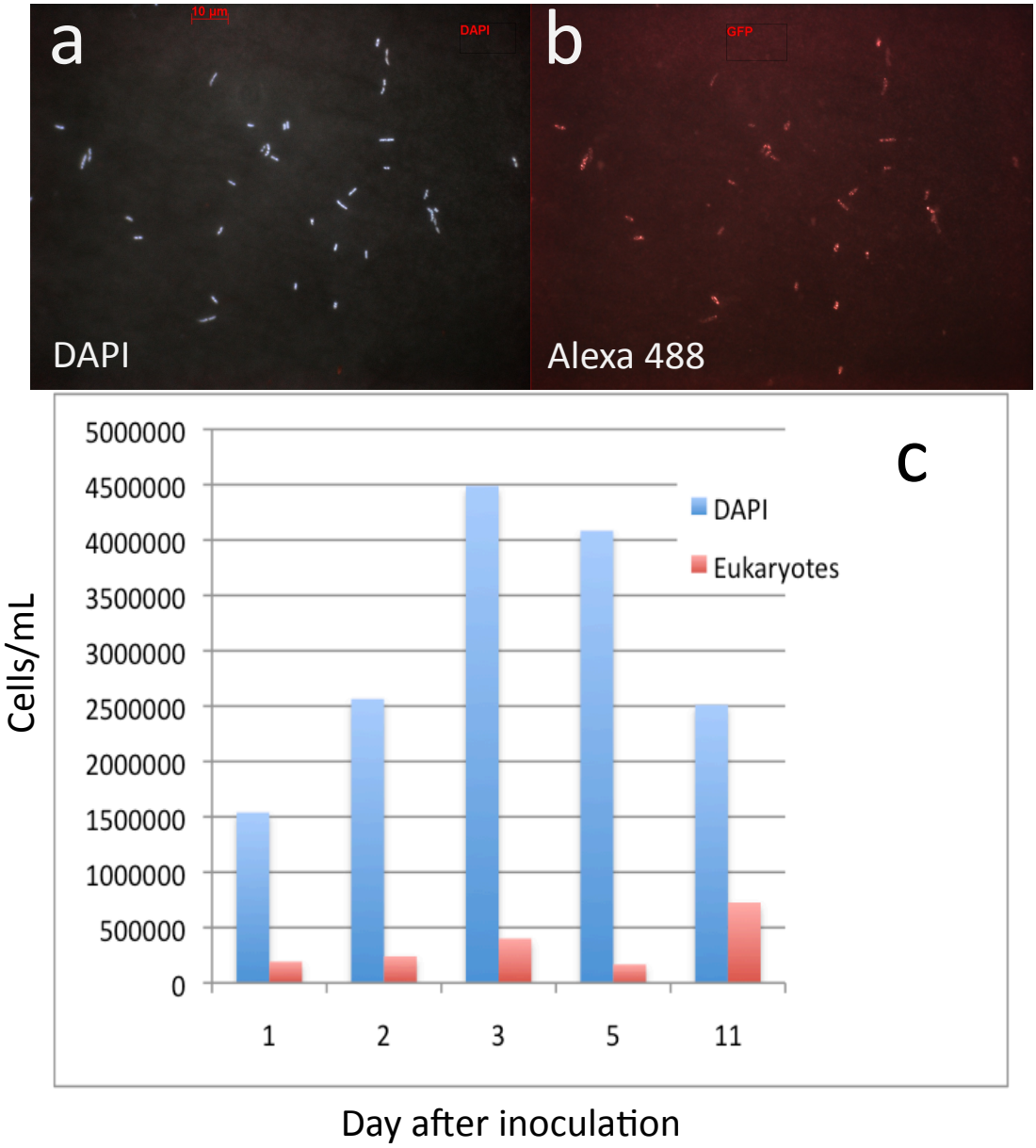

Figure 4. Cell counts by DAPI staining through time. **a)** DAPI and **b)** CARD-FISH with alpha-Proteobacteria probe Alf968 and Alexa 488 was used to confirm that all observed bacterial cells observed belong to alpha-Proteobacteria. Therefore, DAPI was used for total cell counting and identification of Eukaryotes by nuclear staining. **c)** Blue bars are total cell counts (bacteria and Eukaryotes), and red bars are total Eukaryotic cells.

Figure 5

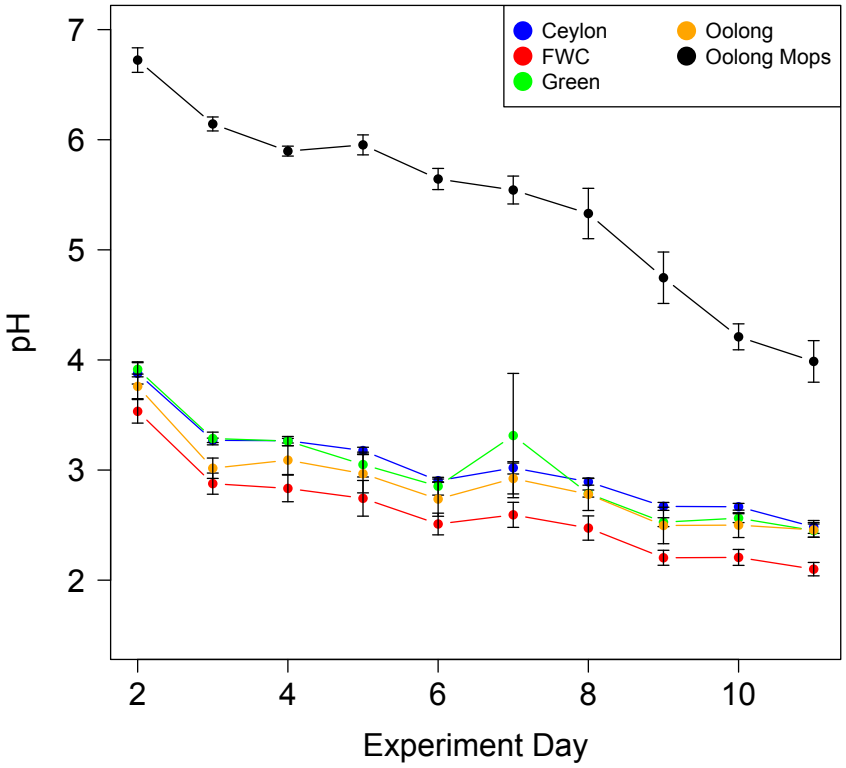

Figure 5. pH dynamics of different treatments to understand the influence of tea origin and pH on the kombucha microbial consortia. Error bars are standard deviations around the mean of three replicates per time point per treatment.

Figure 6

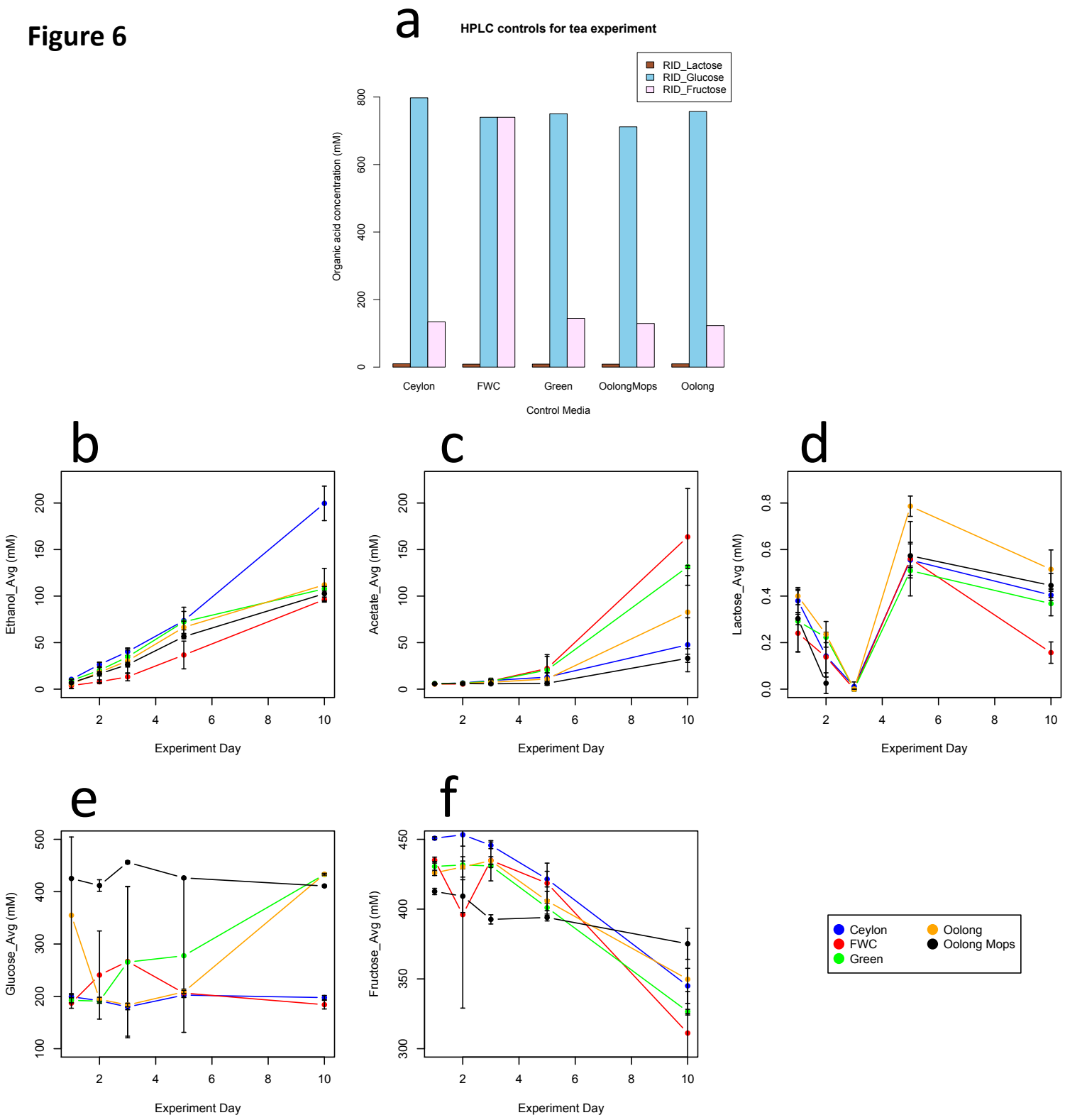

Figure 6. Organic acids analysis by HPLC to understand the influence of tea origin and pH on the kombucha microbial products. **a)** Initial control concentrations of sugars. No acetic acid or ethanol was detected in the controls. **b)** Ethanol; **c)** acetic acid; **d)** lactose; **e)** glucose; **f)** fructose concentrations through time. Error bars are standard deviations around the mean of three replicates per time point per treatment.

Figure 7

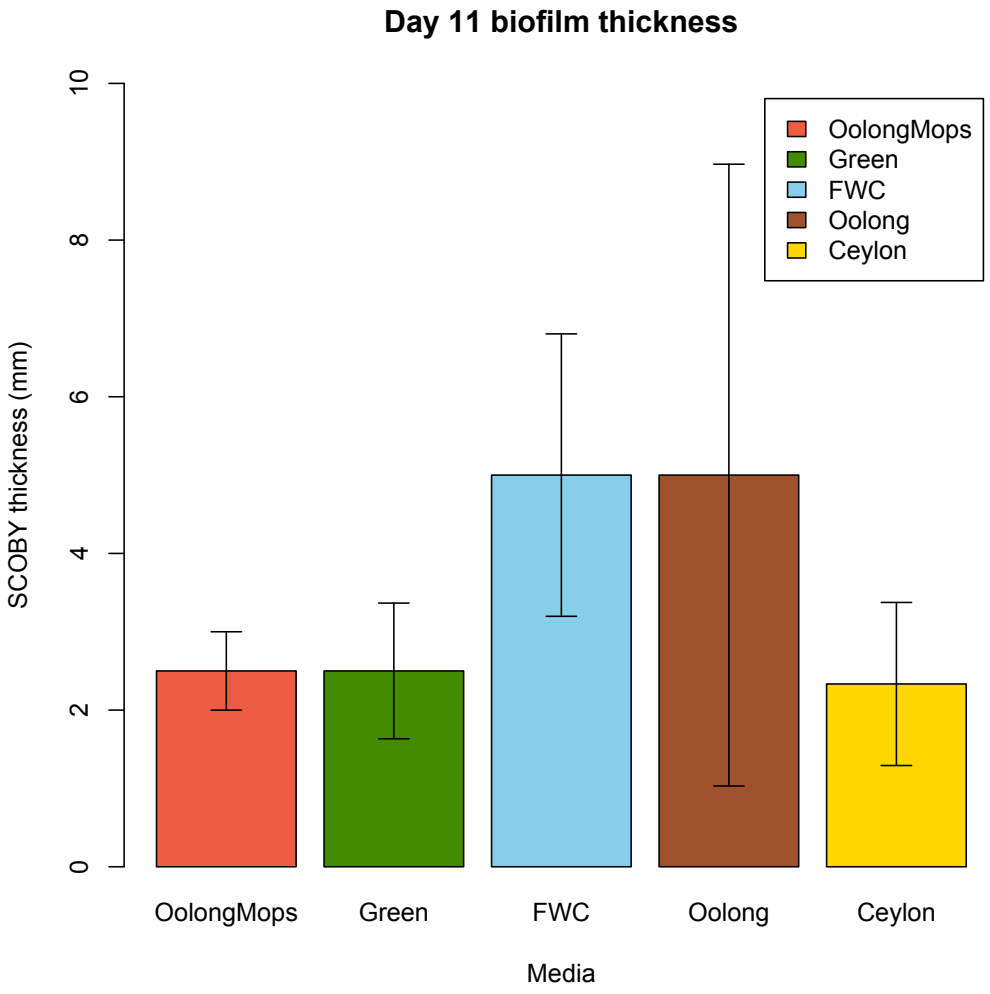

Figure 7. Thickness of biofilms formed by the end of eleven days, as a proxy for cellulose production and biofilm growth. Measurements were at the thickest point in the biofilm.